Asphaltene Precipitation and Deposition under Miscible and Immiscible Carbon Dioxide Gas Injection in Nanoshale Pore Structure

Mukhtar Elturki[1] and Abdulmohsin Imqam[1]*

[1]Missouri University of Science and Technology

Summary

Asphaltene precipitation and deposition is considered one of the prevailing issues during carbon dioxide (CO_2) gas injection in gas enhanced oil recovery techniques, which leads to pore plugging, oil recovery reduction, and damaged surface and subsurface equipment. This research provides a comprehensive investigation of the effect of immiscible and miscible CO_2 gas injection in nanopore shale structures on asphaltene instability in crude oil. A slimtube was used to determine the minimum miscibility pressure (MMP) of the CO_2. This step is important to ensure that the immiscible and miscible conditions will be achieved during the filtration experiments. For the filtration experiments, nanocomposite filter paper membranes were used to mimic the unconventional shale pore structure, and a specially designed filtration apparatus was used to accommodate the filter paper membranes. The uniform distribution (i.e., same pore size filters) was used to illustrate the influence of the ideal shale reservoir structure and to provide an idea on how asphaltene will deposit when utilizing the heterogeneous distribution (i.e., various pore size filters) that depicts the real shale structure. The factors investigated include immiscible and miscible CO_2 injection pressures, temperature, CO_2 soaking time, and pore size structure heterogeneity. Visualization tests were undertaken after the filtration experiments to provide a clear picture of the asphaltene precipitation and deposition process over time. The results showed an increase in asphaltene weight precent in all experiments of the filtration tests. The severity of asphaltene aggregations was observed at a higher rate under miscible CO_2 injection. It was observed that the miscible conditions have a higher impact on asphaltene instability compared to immiscible conditions. The results revealed that the asphaltene deposition was almost equal across all the paper membranes for each pressure used when using a uniform distribution. Higher asphaltene weight percent were determined on smaller pore structures of the membranes when using heterogeneous distribution. Soaking time results revealed that increasing the soaking time resulted in an increase in asphaltene weight precent, especially for 60 and 120 minutes. Visualization tests showed that after 1 hour, the asphaltene clusters started to precipitate and could be seen in the uppermost section of the test tubes and were fully deposited after 12 hours with less clusters found in the supernatant. Also, smaller pore size of filter membranes showed higher asphaltene weight percent after the visualization test. Chromatography analysis provided further evaluation on how asphaltene was reduced though the filtration experiments. Microscopy and scanning electron microscopy (SEM) imaging of the filter paper membranes showed the severity of pore plugging in the structure of the membranes. This research highlights the impact of CO_2 injection on asphaltene instability in crude oil in nanopore structures under immiscible and miscible conditions. The findings in this research can be used for further research of asphaltene deposition under gas injection and to scale up the results for better understanding of the main factors that may influence asphaltene aggregation in real shale unconventional reservoirs.

Introduction

Gas injection has become a promising technique to enhance the oil recovery from unconventional resources, and the results reveal a positive impact on increasing the oil recovery (Elwegaa and Emadi 2019; Altawati 2016; Biheri and Imqam 2020, 2021a; Zheng et al. 2021; Elturki et al. 2021). Even though hydraulic fracturing in horizontal wells was utilized to extract the remaining oil from unconventional reservoirs, only a very small percent can be recovered and the production declines after a few months due to the ultrasmall permeability (Sheng 2015; Zoback and Kohli 2019; Biheri and Imqam 2021b, 2021c; Liu et al. 2021). During multiphase flow production, many problems with multiphase fluids (i.e., gas, oil, condensate, and water) with scale are possible, which could lead to wax and asphaltene deposition, formation hydrates, emulsions, and slugging (Shi et al. 2021). Deposition of organic hydrocarbon solids in oil and gas reservoirs could cause many flow assurance problems during the oil and gas production process. These materials could increase the flow resistance and disrupt production or even plug the pipelines (Hassanpouryouzband et al. 2020; Ali et al. 2021). One of the major problems during gas injection in unconventional resources is asphaltene instability in crude oil. Normally, three main components in crude oil can be found in different percents, which are liquids, dissolved gases, and solids; however, the most common solid in crude oil is asphaltene (Fakher and Imqam 2019; Elturki and Imqam 2020a). Saturates, aromatics, resins, and asphaltenes analysis is used to characterize the crude oil elements. Asphaltene can be defined as "the heaviest component of petroleum fluids that is insoluble in light *n*-alkanes such as *n*-pentane or *n*-heptane, but soluble in aromatics such as toluene" (Goual 2012). Heavier *n*-alkanes precipitate less asphaltene than lighter *n*-alkanes (Behbahani et al. 2011). Asphaltene can be found in colloidal suspensions stabilized by the presence of resins or in solution under reservoir pressure and temperature conditions (Punase et al. 2016; Ali et al. 2021). Changes in reservoir conditions, such as pressure or temperature, lead to asphaltene instability and thus asphaltene deposition and precipitation on solid surface during oil production process (Kar et al. 2020; Mohammed et al. 2021). This phenomenon would cause porosity and permeability reduction, wettability alteration in the reservoir, and subsurface and surface equipment blockages (Madhi et al. 2018; Alimohammadi et al. 2019) and is costly to treat (Melendez-Alvarez et al. 2016; Abutaqiya et al. 2019). CO_2 and nitrogen (N_2) may produce asphaltene flocculation in the reservoir to varying degrees. CO_2 has a high solubility in crude oil and may quickly reach supercritical levels in reservoirs (Wang et al. 2018). Thus, the mass

*Corresponding author; email: aimqam@mst.edu

Original SPE manuscript received for review 23 March 2022. Revised manuscript received for review 30 May 2022. Paper (SPE 210592) peer approved 13 June 2022.

transfer ability of supercritical CO_2 is strong. In the CO_2 injection process, the CO_2-crude oil system could easily reach a miscible or near-miscible state that enhances and extracts the light hydrocarbon components from crude oil into the gas phase. N_2 has weaker solubility in crude oil than CO_2 in the same thermodynamic conditions. Consequently, N_2 has a weak mass transfer capacity which could lead to the poor extraction of light hydrocarbons and probably less asphaltene flocculation compared to CO_2 (Chung 1992; Wang et al. 2018). Under gas injection, asphaltene aggregations can form clusters that may cause critical issues during oil production and thus impact the oil recovery negatively. Understanding the main factors that may affect the asphaltene instability in crude oil during gas injection is extremely important to determine how gas injection flow assurance problems can be avoided in future unconventional enhanced oil recovery applications.

CO_2 gas injection has been widely used to increase oil recovery from both conventional and unconventional resources (Luo et al. 2017; Elturki and Imqam 2020b; Milad et al. 2021). Asphaltene instability during CO_2 and N_2 injection has been studied by many researchers using experimental studies (Jamaluddin et al. 2002; Negahban et al. 2005; Alizadeh et al. 2011; Jafari Behbahani et al. 2012; Moradi et al. 2012; Zanganeh et al. 2018, 2012; Soroush et al. 2014; Shen and Sheng 2018; Fakher and Imqam 2018, 2019, 2020; Guzmán et al. 2020; Elturki and Imqam 2021a, 2021b, 2022a, 2022b; Afra et al. 2020; Nascimento et al. 2021; Espinoza Mejia et al. 2022) and numerical/modeling techniques (Tavakkoli et al. 2014; Alimohammadi et al. 2017; Hajizadeh et al. 2020; Syed et al. 2020; Su et al. 2021; Carvalhal et al. 2021). Negahban et al. (2005) evaluated the asphaltene instability in the reservoir fluids during CO_2 and hydrocarbon gas injection. Results showed an increase in asphaltene precipitation when more hydrocarbon gas was injected. Asphaltene instability was observed during CO_2 injection when increasing the temperature. Using a cubic-plus-association equation of state (CPA-EOS); Li and Firoozabadi (2010) investigated the effects of pressure, temperature, and composition on asphaltene precipitation in several live oils. They mainly studied the effect of pressure decrease and mixing with CO_2 at high temperature and pressure. The tests on the quantity and onset pressures of asphaltene precipitation in different living oils over a wide variety of compositions, temperatures, and pressure conditions were reproduced. They successfully reproduced the asphaltene precipitation envelop; as the temperature is less than 400 K, the temperature shift has a significant effect on the upper onset pressure, according to their findings. The upper onset pressure decreases by 1300 bar as the temperature rises from 300 to 400 K. Once the temperature exceeds 400 K, the temperature's influence on the upper onset pressure becomes low. In comparing to the upper onset pressure, the bubblepoint pressure and lower onset pressure are very poorly temperature dependent. Espinoza Mejia et al. (2022) investigated the phase behavior of asphaltenes instability experimentally. They revealed that when CO_2 concentration increased, the lower asphaltene onset pressure increased in all situations. They also suggested that higher temperatures are advantageous conditions for minimizing asphaltene deposition for the CO_2 injection fraction of 25 to 35%, and temperature and CO_2 fraction are the main controlling factors. On the other hand, the main factor controlling the asphaltene deposition is the CO_2 injection proportion when the fraction ranged from 35 to 45%. To investigate the influence of temperature on asphaltene precipitation and aggregation in light live oils, Mohammadi et al. (2016) conducted several high-pressure, high-temperature depressurization tests. They revealed that depressurization at higher temperatures resulted in higher asphaltene onset pressures or early asphaltene formation. Alves et al. (2019) investigated the influence of temperature on different Brazilian crude oils and observed that as temperature increased, asphaltene precipitation decreased but asphaltene onset increased. Moradi et al. (2012) conducted laboratory experiments to evaluate the asphaltene particle precipitation and aggregation under natural depletion and N_2 injection using high-pressure filtration. The results highlighted that an extreme asphaltene destabilization was observed under N_2 injection. Also, the asphaltene fluctuation masses grew and became more organized when the aggregation of cluster increased. Jafari Behbahani et al. (2012) proposed and conducted a set of experiments using bottomhole live oil sample during CO_2 flooding to study the effect of CO_2 injection on oil recovery and permeability reduction. The cyclohexane and toluene reverse flooding was conducted, and the asphaltene deposition amount was measured by spectrophotometer. Their findings demonstrate that increasing the CO_2 injection pressure led to a significant increase in pressure drop, which resulted in more asphaltene deposition and permeability reduction. Soroush et al. (2014) investigated experimentally, using a coreflooding method, the effect of miscible and immiscible CO_2 injection on asphaltene deposition in porous media. Their observations highlighted that the asphaltene content in the produced oil decreased when increasing the pressure. The results showed that the damage during immiscible injection was due to gas trapping in the pores while during the miscible conditions the asphaltene was responsible for the damage along the cores. Fakher and Imqam (2019) performed an extensive experimental study to evaluate asphaltene deposition and precipitation under CO_2 gas injection using nanocomposite filter membranes. Various factors were evaluated, such as CO_2 injection pressure, oil viscosity, soaking time, and heterogeneity. Their conclusion revealed that as the pressure increased, the asphaltene weight percent for the produced oil increased. Higher temperature resulted in higher asphaltene weight percent for the bypassed oil, and the asphaltene weight percent was reduced when increasing the pore size of the filter membranes. Elturki and Imqam (2021a) conducted experiments using the filtration technique to highlight the effect of immiscible N_2 injection on asphaltene instability. They used various filter membrane papers (i.e., 450, 100, and 50 nm) to mimic the structure of unconventional reservoir structure. First, the slimtube technique was used to determine the N_2 MMP. Based on their results, increasing the pressure led to an increase in asphaltene weight percent, and decreasing the filter membrane pore size increased the asphaltene weight percent significantly. Pore size distribution of the filter paper membrane after the filtration experiments showed a decrease in the pore size due to asphaltene particles. Guzmán et al. (2020) evaluated the asphaltene stability of various Mexican crude oils (API 10 to 52) using spot test, S-value, and static stability test column. Their results showed no uniform results of the stability using different methodologies. Four crude oil samples were used by Afra et al. (2020) to study the effect of CO_2 injection on the structure and stability of asphaltene. Their results showed that, using infrared spectroscopy and acid/base identification, asphaltene stability was disturbed when the amine group of one of the tested asphaltene samples formed an amide functional group by reacting with CO_2. Their study suggested that asphaltene in oil matrix can be destabilized through both chemical reactions and physical interactions. Khalaf and Mansoori (2019) performed a simulation study to evaluate different asphaltenes in different concentrations under N_2 and air injection. The concentration of the injected gas affected the asphaltene aggregation process significantly. The results showed that the asphaltene architecture played an essential role in the process of asphaltene aggregation and significant differences between using N_2 and air on asphaltene aggregations during enhanced oil recovery. Carvalhal et al. (2021) modeled asphaltene precipitation and deposition by evaluating different factors, and the results showed that the thermodynamic sources had more effect on the performance of the model compared to kinetics parameters, which include asphaltene molar content, binary interaction parameters, reference pressure, asphaltene molar volume, surface deposition rate coefficient, and flocculation parameters.

Although several researchers have studied the effect of CO_2 injection on asphaltene deposition and precipitation using multiple methods, few have evaluated both miscible and immiscible CO_2 gas injection and its effect on asphaltene stability in nanopore structures, mainly present in unconventional reservoirs. This research aims to extend the previous work conducted by Elturki and Imqam (2021a), which investigated the impact of immiscible and miscible N_2 injection on asphaltene deposition and precipitation. This research investigated the effect of immiscible and miscible CO_2 gas injection on asphaltene instability in crude oil using nanocomposite filter membranes. This research then quantifies the asphaltene content in all filter membranes under various factors and provides a holistic view on the

impact of various factors. The studied factors include injection pressure, temperature, pore size heterogeneity, and soaking time. The process of asphaltene precipitation and deposition process was presented by the visualization tests. Understating the behavior of asphaltene deposition under CO_2 gas injection is extremely important in unconventional enhanced oil recovery process to avoid any asphaltene problems in both surface and subsurface equipment during production operation.

Experimental Scope Description

The experiments were designed to be conducted in both miscible and immiscible CO_2 gas injection. **Fig. 1** shows the experiment flow chart design in this research, which includes three main tests: (1) MMP determination, (2) filtration, and (3) asphaltene visualization. Further investigations were conducted, such as chromatography analysis, microscopy imaging, and SEM analysis, to highlight the effect of CO_2 gas injection on asphaltene instability in the crude oil and to show the effect of asphaltene particles on pore plugging.

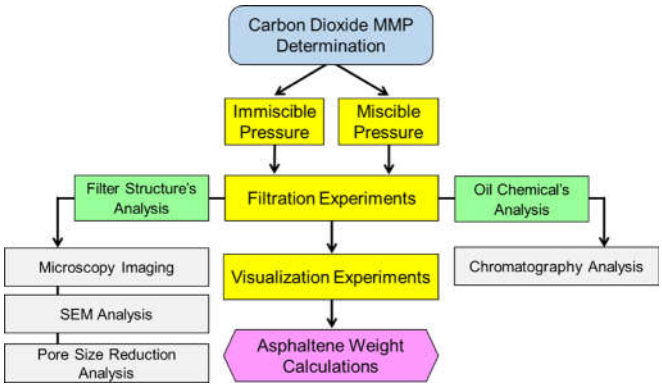

Fig. 1—Experimental design flow chart.

Experimental Materials. The materials used in this research include crude oil with a viscosity of 19 cp, density of 0.864 g/cm^3, and API of 32. A rheometer was used to measure the viscosity of the crude oil. Gas chromatography-mass spectrometry determined the composition of the crude oil, as shown in **Table 1.** Filter paper membranes (i.e., 50, 100, and 450 nm) were used to mimic the unconventional reservoir pore structure and to investigate the effect of various pore sizes. The selection of filter membrane pore sizes was based on the pore size distribution of shale reservoirs, specifically Eagle Ford (Shen and Sheng 2017). The membranes were cut to the desired shape based on the 45 mm diameter of the filtration vessel. A high-pressure, high-temperature stainless-steel vessel was used to accommodate the filter paper membranes. The filtration vessel had a length of 15.24 cm, with inside and outside diameters of 5 and 7.62 cm, respectively. To supply the CO_2 gas injection, a high-pressure CO_2 cylinder was used with a purity of 99.99% and connected to the vessel. A pressure regulator was installed on the cylinder to control the injected pressure. To investigate various temperatures, an oven was used to adjust the temperate during the gas injection. The oven was manufactured by Despatch [Model: LBB2-27-2, Chamber dimensions: 94(width)×94(depth)×89(height) cm]. For the MMP determination, a slimtube made of stainless steel and packed with sand was used. The slimtube had a weight of 2211 g with a length of 13.1 m (inside and outside diameters were 0.21 and 0.41 cm, respectively). The solvent of *n*-heptane was selected to be mixed with the crude oil samples after the filtration experiments in the test tubes to quantify the asphaltene weight percent to determine which asphaltenes are insoluble in *n*-heptane.

Component	Weight Percent (%)
C_8	64.55
C_9	0.28
C_{14}	0.31
C_{15}	0.35
C_{16}	0.43
C_{17}	3.92
C_{18}	0.20
C_{19}	1.17
C_{20}	3.60
C_{21}	0.93
C_{22}	2.66
C_{24}	1.97
C_{27}	5.94
C_{28}	7.22
C_{29}	1.32

Table 1—Grouped carbon number distributions of the original oil.

Component	Weight Percent (%)
C_{30}	1.07
C_{31}	0.53
C_{32}	0.76
C_{33}	0.57
C_{34}	0.59
C_{35}	0.64
C_{37}	0.31
C_{38}	0.38
C_{40}	0.32
Total	100

Table 1 (continued)—Grouped carbon number distributions of the original oil.

Slimtube Experiments. The slimtube technique was selected to determine the MMP of CO_2, which has been used for years to measure MMP because it simulates the 1D displacement of reservoir oil (Amao et al. 2012; Ekundayo and Ghedan 2013; Elturki and Imqam 2021c). The MMP can be defined as the lowest pressure at which the miscibility of gas can be created with the reservoir oil at the reservoir temperature. The miscibility can be achieved when the interfacial tension between the oil and gas vanishes after multiple contacts. The main components of the MMP experiment include a syringe pump, three accumulators, gas cylinders, a stainless-steel slimtube packed with sand, and a backpressure regulator. The first step was a pretest to calculate the pore volume (PV). In the second step, the slimtube was filled with crude oil at a low rate of 0.5 PV to ensure that the slimtube was 100% saturated at the end of pumping. The final step involved experimental manipulation, whereby the temperature was adjusted to a predefined level, the gas cylinder was filled with CO_2, and gas was pumped at a rate of 0.25 mL/min. A backpressure regulator was installed at the outlet of the slimtube and used to adjust the pressure by using another water pump as a backpressure reservoir. **Fig. 2** shows a schematic diagram of the slimtube experimental setup.

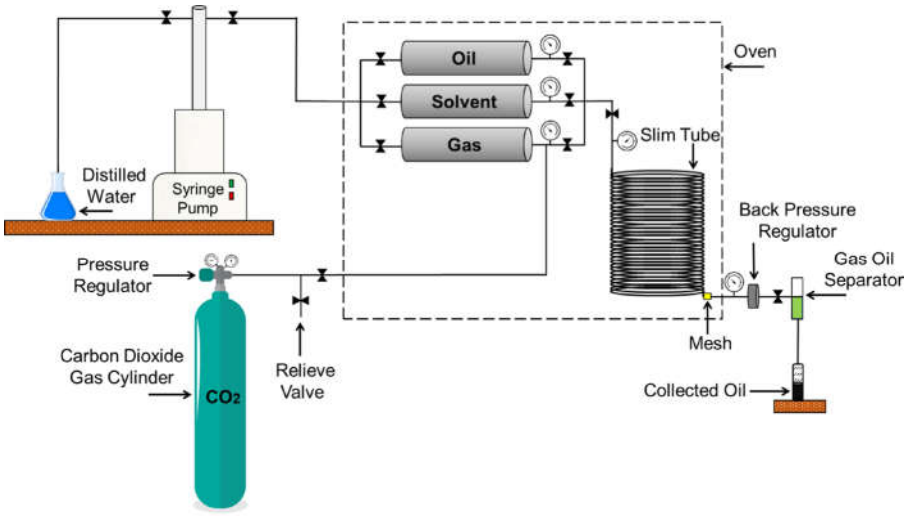

Fig. 2—Schematic of the setup of the CO_2 MMP determination apparatus using the slimtube technique.

The procedure of MMP determination was as follows. The slimtube was fully saturated with the distilled water, and then the oil was injected into the slimtube unit fully saturated. This was observed at the outlet of the slimtube when the produced liquids were only oil, ensuring the slimtube is fully saturated. During all the experiments, the backpressure regulator was placed at the outlet with the desired pressure. The gas accumulator was filled with CO_2. Then, CO_2 was injected at a rate of 0.25 mL/min. Each experiment was stopped when 1.2 PV of gas was injected or when the gas broke through. The effluent was used to collect the produced oil. The MMP was to be determined by plotting CO_2 injection pressures vs. cumulative oil recoveries. Finally, the solvent of xylene was used after each experiment to clean the slimtube setup and to make sure there was no oil left in the slimtube that could affect the next experiment.

Filtration Experiments. The components of the filtration setup are shown in **Fig. 3.** The main components included a high-purity CO_2 cylinder with a pressure regulator to control the pressure from the cylinder. The gas accumulator was used to accumulate the CO_2 gas and inject it into the vessel using a syringe pump to reach higher pressures due to the limitation of outlet pressure in the CO_2 cylinder. The high-pressure, high-temperature filtration vessel **(Fig. 4a)** was designed to accommodate three mesh screens to support the filter membranes and prevent them from folding under high pressure. The mesh screens were designed with small holes that allowed the oil to pass through easily, as shown in **Fig. 4b**. Spacers between each mesh screen were added to support each mesh screen in its place, and rubber O-rings were used above and below each spacer to prevent leakage and to ensure that the oil and gas would pass through the filter paper membranes. A backpressure regulator was installed at the outlet of the filtration vessel and used to adjust the pressure using

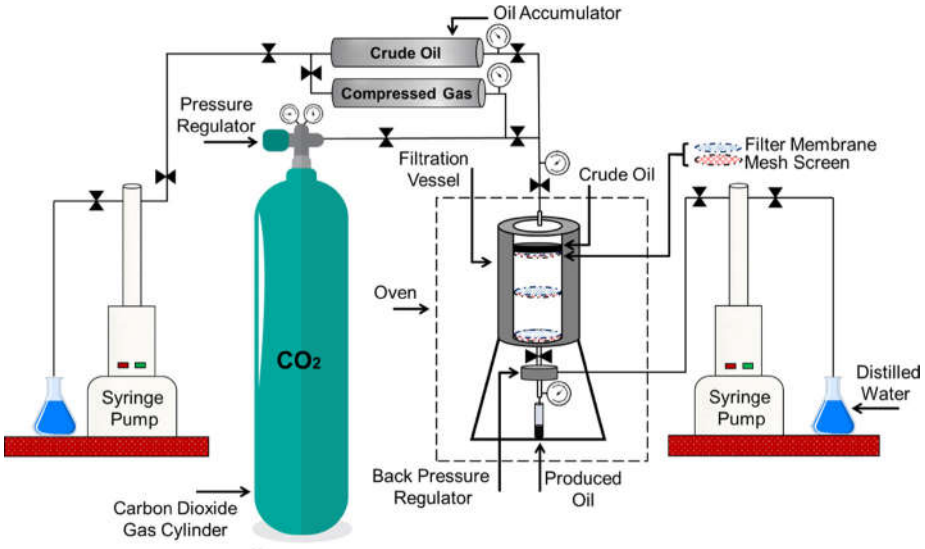

Fig. 3—Filtration experiments setup.

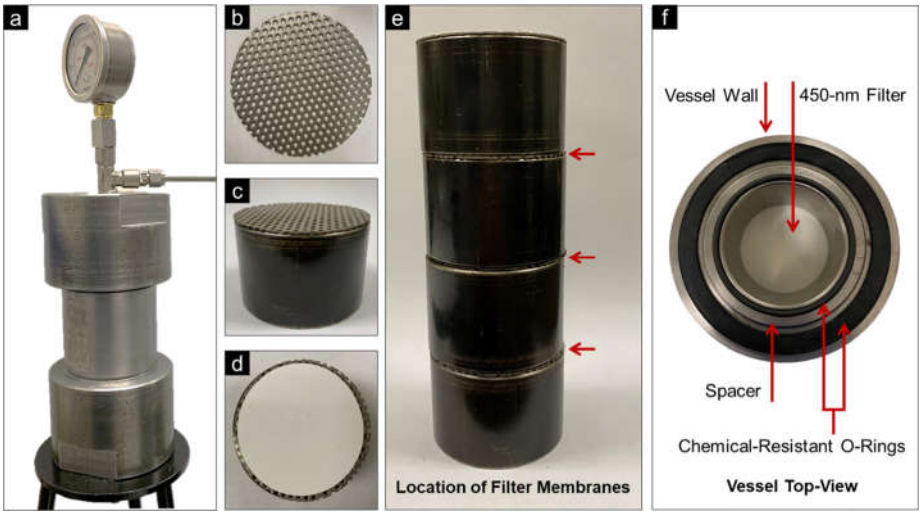

Fig. 4—Filtration vessel equipment include (a) real filtration vessel, (b) mesh screen, (c) mesh screen on top of spacer, (d) top view of filter membrane on top of mesh screen and spacer, (e) four stainless-steel spacers used inside the filtration vessel and the arrows indicate the location of the filter paper membranes, (f) vessel top view showing the 450-nm filter inside the vessel when using the heterogenous distribution.

a syringe pump. The produced oil was collected using an effluent below the filtration vessel for further analysis. An oven controlled the temperature of the filtration vessel to study the effect of different temperatures. Finally, two transducers were installed at the inlet and outlet of the filtration vessel and were connected to a computer to monitor and record the pressure differences.

The first set of mesh screens along with a filter membrane paper, rubber O-ring, and spacer were placed inside the filtration vessel in that order. This step was repeated with the next two sets, after which the vessel was closed using a specially designed cap that ensured a tight connection between all the sets and prevented leakage during the experiment. An oil accumulator injected 30 mL of crude oil into the vessel using a syringe pump. Next, the CO_2 cylinder injected gas into the vessel to the desired pressure level and exposed the crude oil to the gas for a specific soaking time. Then, the syringe pump at the outlet was turned to constant pressure but was adjusted to the required backpressure for each experiment to let the crude oil pass through the membranes. CO_2 was injected continuously into the vessel, and the produced oil was collected for further analysis (e.g., chromatography analysis). The experiment was stopped when no further oil production was observed. During the experiment, the inlet and outlet pressures were recorded using transducers connected to a computer. The difference between the two pressures did not exceed 50 psi. After the experiment, the vessel was opened, and the trapped crude oil was collected from each filter membrane for analysis. Finally, in preparation for the next experiment, the solvent *n*-heptane was used to clean the vessel, mesh screens, and spacers of precipitated and deposited oil.

Asphaltene Visualization and Detection Tests. The visualization tests were conducted to highlight the asphaltene precipitation and deposition process at various conditions. Then, the asphaltene percent was quantified using the standard test (IP 143) of the *n*-heptane insoluble asphaltene content determination in crude oil (Shahriar 2014). The visualization test was conducted by first placing in a test tube 1 mL of crude oil collected from all filter membranes, the produced oil, and the remaining oil from the filtration experiments. The oil was

then collected using a pipette to ensure the accuracy of all samples. Second, 40 mL of *n*-heptane was added to each test tube. Tubes were closed tightly to prevent *n*-heptane evaporation. Each test tube was shaken well to ensure that the *n*-heptane was well dispersed within the crude oil. A special laboratory stand was used to handle the test tubes. The asphaltene then started to settle slowly. Photos were taken at specific time points (i.e., 0, 2, 4, and 12 hours) to observe the change in asphaltene settling over time. A filter paper with 2.7 μm pore size was used to filter the precipitated asphaltenes in the test tube and then to quantify the asphaltene content. Asphaltene weight percent can be calculated by weighing the filter paper before and after the filtration process using a high-precision balance. The difference between these weights determines the asphaltene weight percent using the following equation:

$$\text{Asphaltene wt\%} = \frac{\text{wt asphaltene}}{\text{wt oil}} * 100, \quad (1)$$

where asphaltene wt% is the asphaltene weight percent, wt asphaltene is the asphaltene weight on the filter paper, and wt oil is the oil sample weight. The asphaltene quantification test procedure is summarized in the flow chart shown in **Fig. 5.**

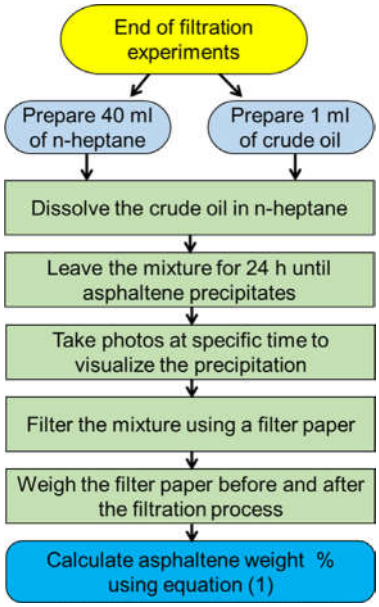

Fig. 5—Flow chart highlighting the main steps of asphaltene visualization tests.

Results and Discussion

MMP Experiments Results. The main mechanism by which CO_2 can achieve miscibility is the vaporizing mechanism. The MMP tests were conducted to ensure that we select the right miscible and immiscible pressure to conduct the filtration experiments. The impact of a high temperature on MMP was investigated to ensure that the filtration experiments were in the right condition of miscible or immiscible at higher temperatures. Oil recoveries were recorded at gas breakthrough or at 1.2 PV of the gas injected and were plotted with the tested injection pressures. When the cumulative oil recovery became higher than or equal to 90% of the initial oil in place, the MMP could be determined, as shown in **Fig. 6. Table 2** shows the cumulative oil recoveries of slimtube tests at temperatures of 32 and 70°C. The solid lines in **Fig. 6** were utilized to establish the point where the observed oil recovery against injection pressure suddenly changed slope.

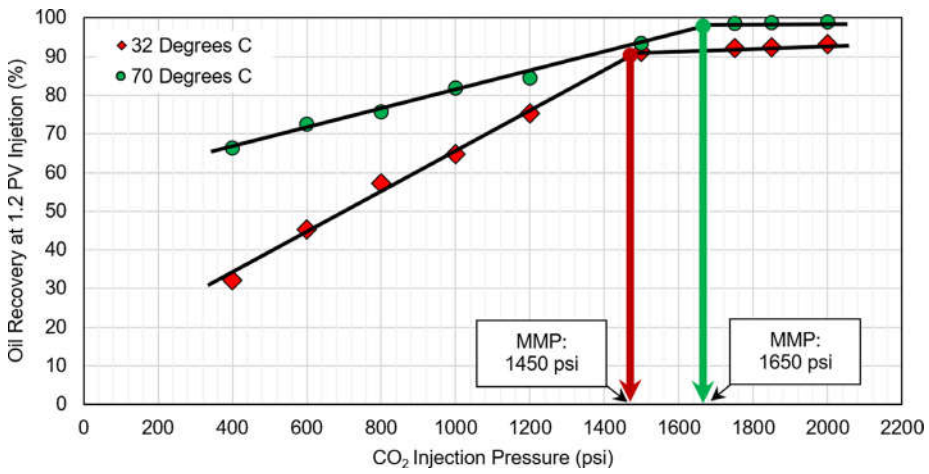

Fig. 6—CO_2 MMP determination using an oil viscosity of 19 cp at 32 and 70°C.

Then, the MMP was determined using the intersection point. At 32°C, the MMP of CO_2 was determined to be 1,450 psi. As a result, for examining asphaltene precipitation and stability under immiscible gas injection condition, pressures of 750, 1,000, and 1,250 psi were chosen, along with a temperature of 32°C. On the other hand, a higher temperature of 70°C resulted in a MMP with 1,650 psi. So, the pressures of 1,500, 1,750, and 2,000 psi were selected to present the miscible condition in the filtration experiments. It was observed that the temperature has a direct relationship with MMP; as the temperature increases, the MMP will increase (Zolghadr et al. 2013).

Tested injected pressure (psi)	400	600	800	1,000	1,200	1,500	1,750	1,850	2,000
Cumulative oil recovery at 32°C	32.20	45.40	57.10	64.71	75.20	91.30	92.10	92.50	93.12
Cumulative oil recovery at 70°C	66.30	72.50	75.60	81.90	84.40	93.30	98.50	98.80	99.10

Table 2—CO_2 slimtube cumulative oil recoveries (%).

Filtration and Visualization Results. ***Effect of Miscible and Immiscible Pressure Using Uniform Membrane Distribution.*** The term "uniform membrane distribution" refers to the use of the same pore size filter membrane in all the filtration experiments. The distribution of the paper membrane inside the vessel is shown in **Fig. 7**, with a pore size of 100 nm for the entire membrane. The selection of filter membrane pore sizes was based on the pore size distribution of shale reservoirs, specifically Eagle Ford (Shen and Sheng 2017). The impact of using a uniform pore size filter paper membrane on the asphaltene deposition during the filtration test is shown in **Fig. 8.** The effect of applying the same pore size was investigated by placing three 100-nm filter membranes inside the vessel in each mesh screen, and the findings were compared to a heterogeneous distribution. CO_2 immiscible pressures of 750, 1,000, and 1,250 psi and miscible pressures of 1,500, 1,750, and 2,000 psi were used to investigate the impact of miscibility on asphaltene disposition. All the experiments were conducted at temperature of 32°C. The results revealed that the asphaltene deposition was almost equal across all the paper membranes for each pressure used. Increasing the pressure increased the asphaltene weight percent in all the experiments. It was observed that the miscible conditions have a higher impact on asphaltene instability compared to immiscible conditions. For instance, the asphaltene weight percent ranged from 7.98% in the upper part of the 100-nm paper membrane to 7.95% in the lower part of the 100-nm paper membrane during the immiscible pressure of 750-psi gas injection. By comparting these findings to the miscible condition of 2,000 psi, the asphaltene weight percent ranged from 19.95% in the upper part of the 100-nm paper membrane to 19.66% in the lower

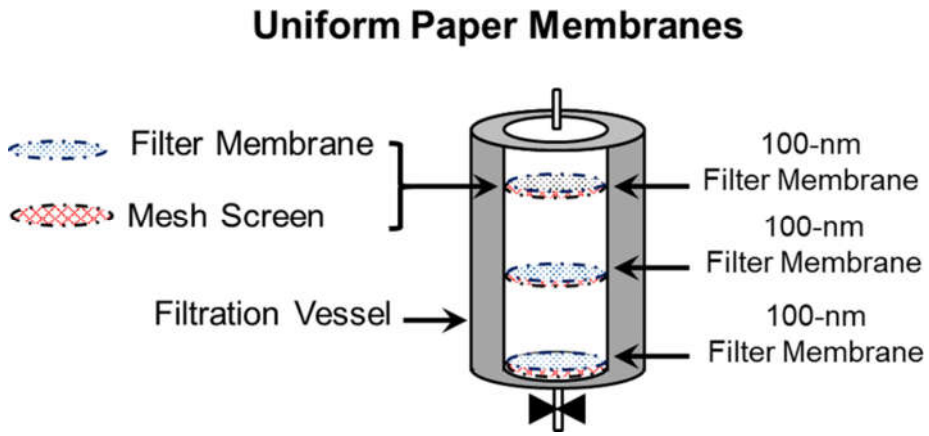

Fig. 7—Illustration of the uniform paper membrane distribution inside the vessel.

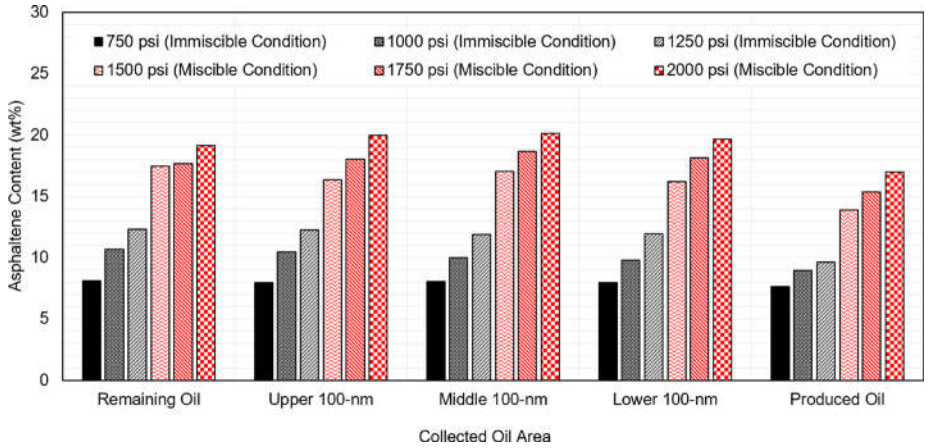

Fig. 8—Asphaltene weight percent distribution using uniform paper membranes with immiscible and miscible CO_2 injections.

part of the 100-nm paper membrane. There is a slight difference between the asphaltene weight percent in all the filter membranes because some asphaltene particles plugged some pores in the middle and the lower membranes during the injection process, thereby affecting the oil passage. These plugged pores resulted in a decrease in the asphaltene weight percent in the produced oil. Asphaltene particles larger than 100 nm precipitated on the upper section of the filter membrane, while particles less than 100 nm went through and were collected with the produced oil. A pressure of 1,750 psi, for instance, created considerably more asphaltene clusters than a pressure of 750 psi as well as more asphaltene deposited on the filter membranes. More clusters of 100 nm or larger were formed as a result of the increased pressure. Thus, more asphaltenes were quantified at higher pressure levels in all filter membranes. In summary, because of the uniform pore size of the filter paper membranes, the asphaltene clusters were forced and deposited into the filter membranes with almost the same concentrations in all the experiments.

A miscible pressure of 1,750 -psi and immiscible pressure of 750 -psi CO_2 injection were selected to investigate the asphaltene precipitation process over time. The remaining oil was collected after each experiment and dissolved in *n*-heptane at a ratio of 1:40. Various times were selected (i.e., 1, 4, and 12 hours) to investigate and visualize the asphaltene deposition process. **Figs. 9a and 9b** show the uniform asphaltene visualization tests at 750 and 1,750 psi with 100-nm pore size membranes at 32°C. There was no asphaltene present at zero elapsed time, and the crude oil sample was completely dissolved in *n*-heptane. The miscible pressure showed a slight dark color of the mixture at zero elapsed time compared to the immiscible pressure. After 1 hour, the asphaltene clusters started to appear and precipitate with a small amount of asphaltene particle in the bottom of the tube. Over time, the color of the top of the laboratory tubes started to be lighter with the presence of some suspended particles of asphaltene. More asphaltene particles can be observed in miscible conditions of 1,750 psi, indicating that miscibility impacts the instability of asphaltene at higher rates. Finally, after 12 hours, almost all asphaltene particles and clusters were deposited in the bottom of the laboratory tube and the color of the solution was much lighter compared to the zero-time observation. The pictures reveal that miscibility had higher impact on asphaltene instability and same pore size distribution led to almost the same precipitation process for all filter paper membranes in both conditions.

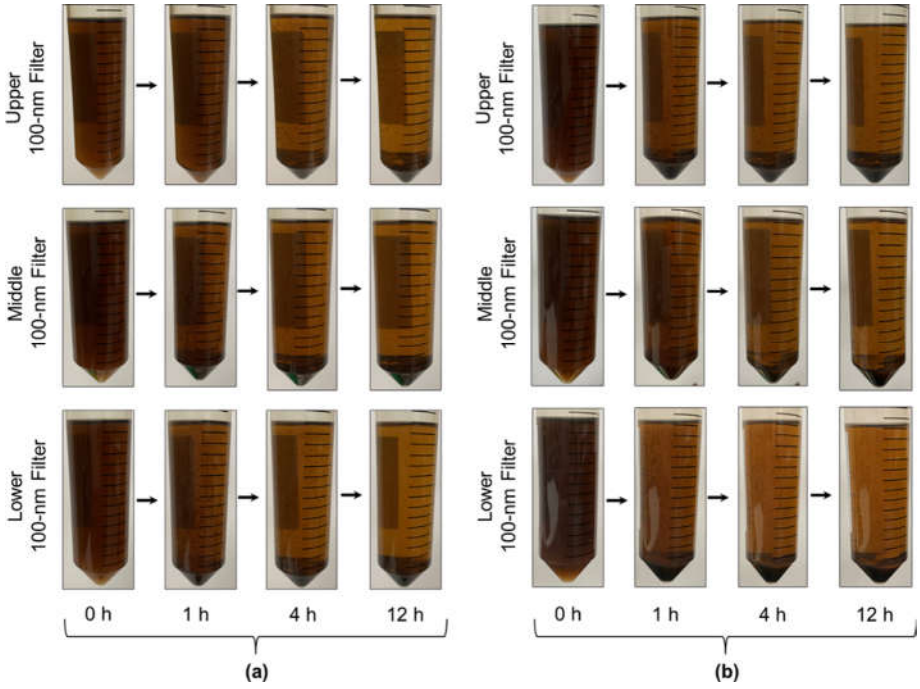

Fig. 9—Visualization of asphaltene precipitation and deposition using a uniform membrane size distribution a: (a) immiscible pressure of 750 psi and (b) miscible pressure of 1,750 psi.

Effect of Pore Size Heterogeneity. **Fig. 10** shows the heterogeneous distribution of the filter membranes, starting with a 450-nm filter in the upper mesh screen, a 100-nm filter in the middle, and a 50-nm filter in the lower mesh screen. As explained in the previous section, miscible pressures (i.e., 1,500, 1,750, and 2,000 psi) and immiscible pressures (i.e., 750, 1,000, and 1,250 psi) were selected to investigate the heterogeneity of the filter paper membranes at 32°C with a 2-hour soaking time. The soaking time effect will be presented in the following sections. The asphaltene weight percent was increased when increasing the pressure and during the miscible conditions due to the resins that connect all the asphaltene particles and solid components in the crude oil when broken down; thus, asphaltene weight percent will increase. **Fig. 11** presents the asphaltene weight percent using a heterogeneous paper membrane distribution during miscible and immiscible CO_2 injection pressures. When using low immiscible 750-psi gas injection, the asphaltene weight percent increased from 7.45 to 9.36% in the 450- and 50-nm filters, respectively. Increasing the pressure to 1,000 and 1,250 psi resulted in a significant increase in asphaltene weight percent in both pressures, especially at 1,250 psi. At 1,250-psi injection pressure, the asphaltene weight percent increased up to 16.97% in 50-nm filter. This revealed that the injected pressure had an effect on the asphaltene particles and clusters, resulting in asphaltene deposition dependent on the asphaltene particle size. Filter membrane pores became almost blocked as a result, particularly in the 50-nm filter. The ability of asphaltene particles to pass through the filter membranes was affected by the size of their pores. The asphaltene aggregates continued to interact with one another because of Brownian motion, producing bigger particles. Smaller aggregates have a stronger tendency to deposit due to the significant radial diffusivity of the particles, which describes the ability of a particle to be pushed by a collision with asphaltene aggregates (Hashmi and Firoozabadi 2010; Hassanpouryouzband et al. 2017). More nanoaggregates combined together and resulted in more clusters, which led to pore plugging in all filter membranes. Injecting higher pressures (i.e., 1,500, 1,750, and 2,000 psi) with miscibility conditions increased the asphaltene weight percent sufficiently. For instance, the weight percent of asphaltene ranged from 13.01 to 20.20% in the 450- and 50-nm filters, respectively. The highest weight percent was

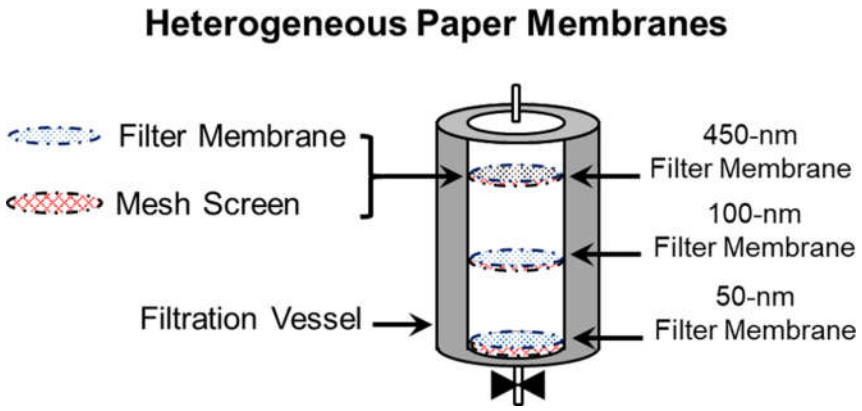

Fig. 10—Illustration of the heterogeneous paper membrane distribution inside the vessel.

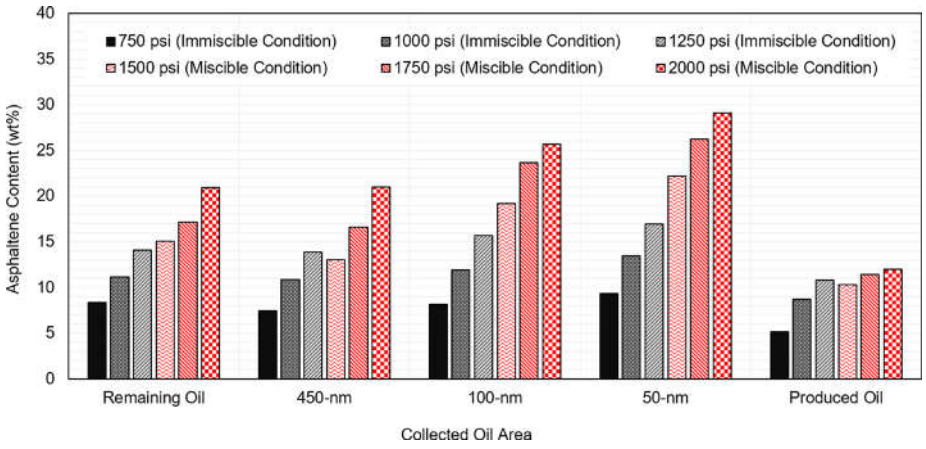

Fig. 11—Asphaltene weight percent using a heterogeneous distribution using miscible and immiscible CO2 injections.

observed at miscible pressure of 2,000 psi, which was 25.47% in 50-nm filter membrane. These results confirm that the miscibility of gas impacts the asphaltene stability in oil in a higher rate compared to immiscible conditions of gas. Also, these findings clearly suggest that asphaltene particles changed the oil's capacity to flow through, which may happen in actual reservoirs and cause serious issues. Because the asphaltene clusters had plugged the pores in all of the filter membranes, the produced oil had a lesser asphaltene weight percent.

After each experiment was completed, the collected oil was analyzed to see the asphaltene deposition and precipitation process over time. The oil collected from 450-, 100-, and 50-nm filter membranes was analyzed under immiscible condition of 750 psi and miscible condition of 1,750 psi, as shown in **Figs. 12a and 12b.** A ratio of 1:40 was used to mix the oil samples with the solvent *n*-heptane in test tubes to observe the precipitation and deposition process over different times (i.e., 0, 1, 4, and 12 hours). The captured photos show that at 0 hour, all the oil samples collected from all filter paper membranes were fully dissolved in *n*-heptane and no asphaltene clusters or particles were observed in both conditions of gas injection (i.e., immiscible and miscible). A slightly lighter color was observed in the test tube of 450-nm filter membranes in both conditions. After 1 hour, the asphaltene particles started to form in the mixture and started to form small clusters, especially in the sample collected from 100- and 50-nm filter membranes. The miscible test tubes showed a slightly darker color due to higher pressure weakening the bonds between asphaltene and resins at a higher rate compared to immiscible conditions. It was interesting to observe that the asphaltene accumulations and deposition were clear in the bottom of the test tube after 4 hours of the oil samples collected from 450-nm filter membranes. Over time, the supernatant became lighter in color and the asphaltene clusters started to settle down and form higher amounts of asphaltenes. After 12 hours, most of the asphaltene particles were settled down and deposited for all oil samples collected from all paper membranes. These findings showed that pressure (i.e., immiscible and miscible) has a substantial impact on the stability of asphaltene. As a result, it is critical to investigate the impact of pressure on asphaltene stability to predict and minimize any problems.

Effect of Soaking Time. To understand the impact of soaking time on asphaltene precipitation and deposition, three separate experiments using 1,000- psi injection pressure with durations of 10, 60, and 120 minutes were selected. The soaking time is when the gas was injected into the vessel at the desired pressure and at 32°C to allow the CO_2 to mix with the crude oil. **Fig. 13** shows the asphaltene weight percent in all filter membranes during various soaking times. The results demonstrated that increasing the soaking time led to an increase in asphaltene weight percent in all filter paper membranes. For example, the asphaltene weight percent in the 450-nm filter increased from 6.26 to 10.14% for 10 and 120 minutes, respectively. Small pore size of the 50-nm filters resulted in an increase in asphaltene weight percent due to the asphaltene clusters plugging the small pores during the filtration process. The bonds between asphaltene and resins in the crude oil were weakened in a lower rate at 10 minutes soaking time, which confirms that, due to time limitation of the soaking process, the asphaltene weight percent was lower compared to 120 minutes. Given these observations, the soaking time had an impact on asphaltene instability in the crude oil, especially for a time longer that 10 minutes. The findings showed that the effect of 60 minutes had similar effect on asphaltene aggregation even though the weight percent was slightly higher at 120 minutes. The longer soaking time investigated was 120 minutes because the difference between the asphaltene weight percent in both 60 and 120 minutes was not significant.

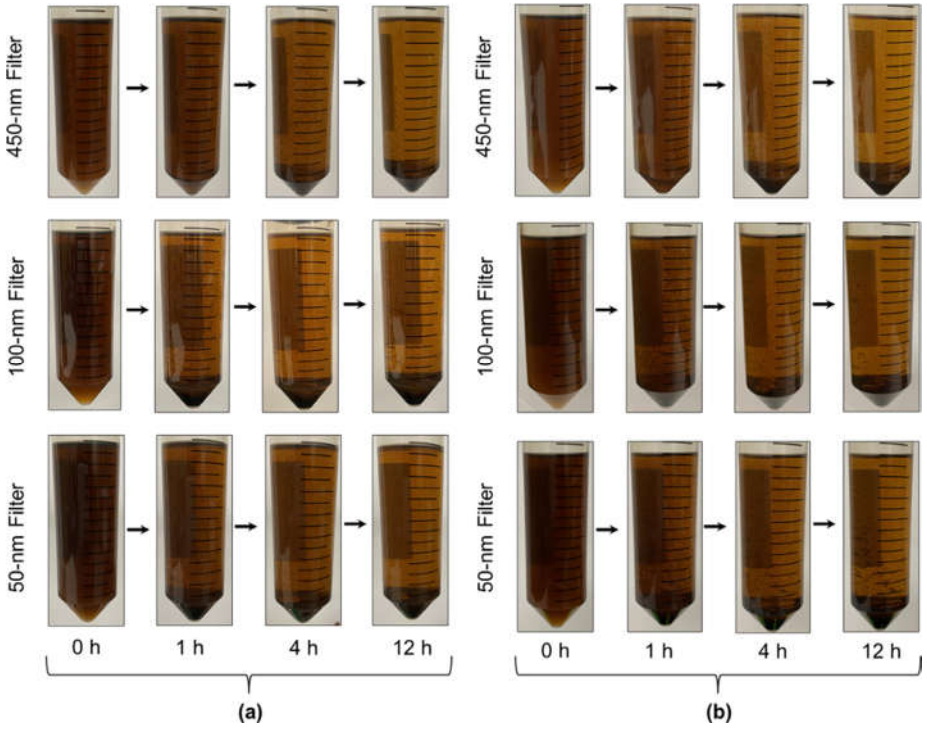

Fig. 12—Visualization of asphaltene precipitation and deposition using a heterogeneous membrane size distribution at (a) immiscible pressure of 750 psi and (b) miscible pressure of 1,750 psi.

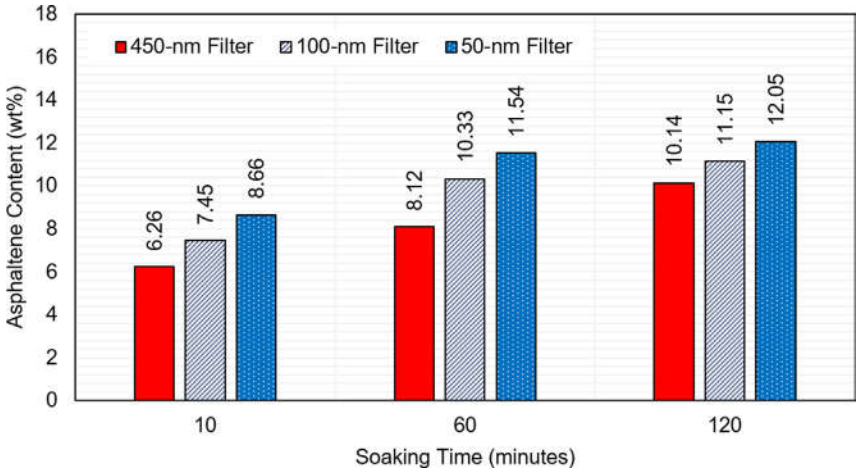

Fig. 13—Asphaltene weight percent at soaking times of 10, 60, and 120 minutes using 450-, 100-, and 50-nm filter membranes.

Effect of Temperature on Asphaltene Deposition. Temperature has a great effect on asphaltene stability in crude oil. To study the influence of a higher temperature on asphaltene stability, two tests were performed at two temperatures (32 and 70°C). The 32°C represents normal temperature, and 70°C represents the average temperature of shale basins. A pressure of 1,000-psi injection and a 2-hour soaking time were used in both experiments to evaluate the temperature impact on asphaltene stability. A heterogeneous filter paper distribution was used in both experiments. Increasing the pressure led to a decrease in asphaltene weight percent in all filter paper membranes, as shown in **Fig. 14.** The higher percent of asphaltene was found in the 50-nm filter paper membranes, which changed from 18.90 to 16.23% for 32 and 70°C, respectively. The suspension colloidal particles of asphaltene in stable oils are covered by resins that are strongly connected to the asphaltene. At higher temperatures, this connection between asphaltene and resins can be stronger and keeps the asphaltene dissolved in the crude oil (Hoepfner et al. 2013). Less asphaltene colloidal is produced at higher temperatures and the associations are weaker due to resins dispersed strongly the collides of asphaltenes (Branco et al. 2001). At higher temperatures, the precipitated asphaltenes created from colloidal suspension particles tend to dissolve in the oil, resulting in the formation of more asphaltenes in soluble conditions but less in colloidal ones (Chandio et al. 2015). Moreover, resins tend to have a strong self-associate like asphaltenes at lower temperatures; thus, the connection between resins and asphaltenes is reduced (Pereira et al. 2007). As a result of these mechanisms, asphaltene aggregates can be formed because of strong polarity and self-association to form aggregates at lower temperatures. It can be concluded that the asphaltene precipitated from the colloidal suspension was dissolved in the crude oil until reaching equilibrium. This resulted in more soluble asphaltenes in oil and less asphaltenes in colloidal form (Chandio et al. 2015). Also, the same observation was noticed for the filter paper pore size in which smaller pore size had higher asphaltene weight percent in both temperatures. This was due

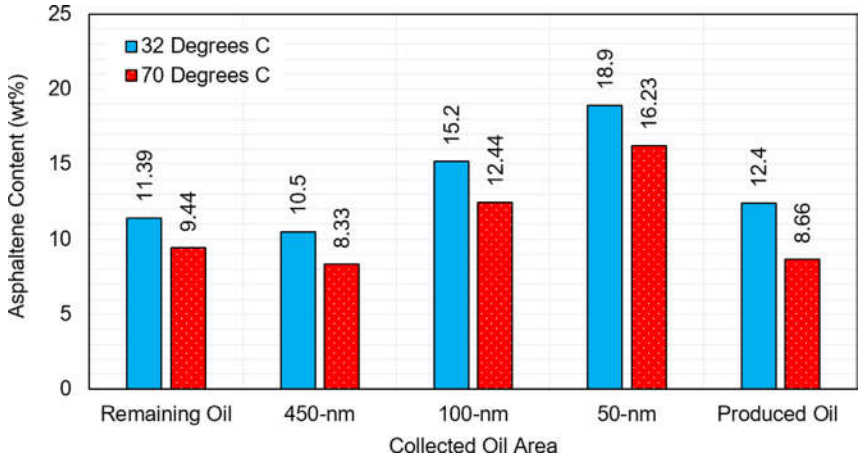

Fig. 14—Asphaltene weight percent at different temperatures during CO_2 injection at 1,000 psi.

to the asphaltene particles plugging the pores of 50-nm filter paper membrane much more compared to 450 and 100 nm; thus, higher asphaltene weight percent was determined.

Further Analysis and Discussion

Chromatography Analysis. Gas chromatography-mass spectrometry (GC6890-MS5973) was utilized to analyze the main chemical components of the crude oil used during the filtration experiments to highlight the chemical structure changes, including asphaltene, after the injection of CO_2. First, the original oil was analyzed before conducting the filtration experiments. Then, the produced oil after the filtration experiments was collected for further analysis. Four produced oils were selected after filtration experiments using pressures of 1,000 and 1,750 psi to investigate the impact of immiscibility and miscibility conditions on the chemical components of crude oil and to show the influence of pore size of filter paper membranes on asphaltene deposition. **Table 3** presents the grouped carbon number distributions before and after CO_2 gas injection filtration experiments at immiscible conditions (i.e., 750 and 1,250 psi) and miscible conditions (i.e., 1,750 and 2,000 psi). The findings showed that the light components (C_8–C_{14}) were partially extracted when using 1,250 psi, which decreased from 52.72 to 47.32% when using 750 and 1,250 psi, respectivelcy. When utilizing miscible gas injections of 1,750 and 2,000 psi, the light components substantially reduced to 40.66 and 30.59 %, respectively. Miscible conditions had higher impact on the crude oil and this can be seen in the higher mole percent of the intermediate and heavy components (C_{15}–C_{30+}). For instance, the heavy components of C_{30+} increased significantlty from 5.38 to 13.50% at immiscible pressure of 750 psi and miscible pressure of 2,000 psi, sequentially. This confirms that asphaltene particles and clusters deposited on the filter paper membranes during the filtration experiment and reduced its content and the heavy components in the produced oil. Increasing the pressure above the MMP resulted in an increase in heavy components and asphaltene content compared to pressure below MMP (i.e., immiscible conditions). These results indicated that miscibility had impacted the crude oil and its chemical structure much more than immiscible gas injection conditions. The strong light-hydrocarbon extraction of miscible CO_2 leads to a higher percent of heavy hydrocarbons and less light and intermediate hydrocarbons (Cao and Gu 2013). Higher pressure of miscibility will force the asphaltene particles and the heavy components to pass through the filter membranes at higher rate and thus result in an increase in the asphaltene content in the produced oil.

		Pressure Condition			
		Immiscible Conditions		Miscible Conditions	
Carbon Number Group	Original Oil Before Experiments	750 psi	1,250 psi	1,750 psi	2,000 psi
C_8 –C_{14}	65.14%	52.72%	47.32%	40.66%	30.59%
C_{15}–C_{19}	6.06%	3.85%	3.50%	8.45%	5.12%
C_{20}–C_{24}	9.16%	16.32%	20.11%	17.45%	20.10%
C_{25}-C_{29}	14.48%	21.74%	22.74%	25.28%	30.69%
C_{30+} (including asphaltene)	5.17%	5.38%	6.33%	8.16%	13.50%
Total	100.00%	100.00%	100.00%	100.00%	100.00%

Table 3—Grouped carbon number distributions of the original oil and the remaining oil after immiscible and miscible CO_2 injection.

Microscopy Imaging Analysis. Asphaltene clusters and aggregations can be formed after CO_2 injection, and these new forms of asphaltene particles can cause severe issues and plug the pores in a reservoir. A reduction in oil recovery and wettability alteration can be encountered during the asphaltene precipitation and deposition process. In this section, a solvent of *n*-heptane was used to clean the filter paper membranes after the filtration experiments to highlight the pore plugging due to asphaltene particle and clusters. **Fig. 15** shows the filter membranes (i.e., 450 and 50 nm) before and after conducting the filtration experiment with 1,500-psi gas injection as well as after cleaning the crude oil from the filter membrane. The photos reveal that the pores were plugged and the asphaltene particles were deposited

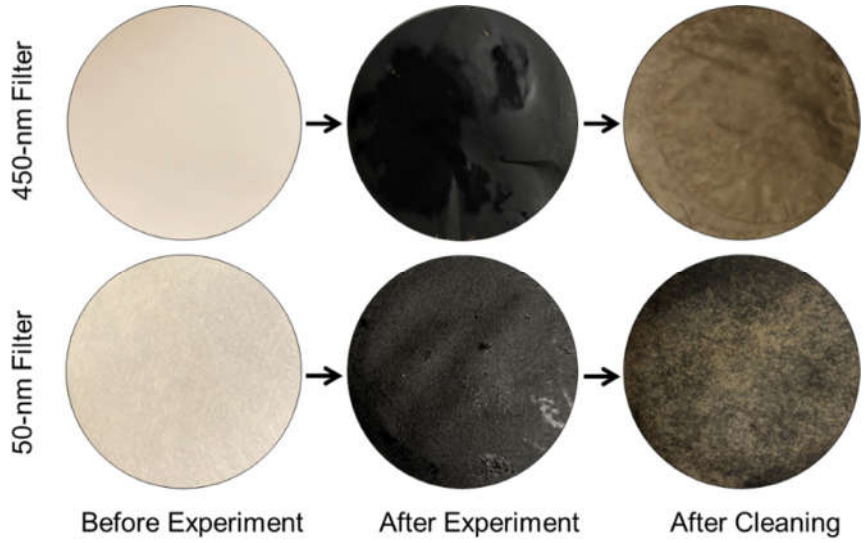

Fig. 15—Illustration of the filter membranes (450 and 50 nm) at 1,500 psi before and after the experiment and after cleaning.

causing a reduction in pore size and oil path in filter paper membranes, especially in the 50-nm filter paper membranes which have smaller pore size. To highlight the severity of pore plugging in all filter paper membranes, a HIROX digital microscope was used to show the plugging pores. The filter paper membranes of a heterogeneous filter distribution of immiscible and miscible filtration experiments were selected for further analysis. **Fig. 16** shows the microscopic images of the filter membrane's pore structure of 450-, 100-, and 50-nm filters using immiscible conditions (i.e., 750, 1,000, and 1,250 psi) and miscible conditions (i.e., 1,500, 1,750, and 2,000 psi) at 32°C. All images were captured after cleaning the filter paper using *n*-heptane solvent for at least 24 hours. It was observed that miscible conditions of CO_2 had higher pore plugging of the filter paper membranes compared to immiscible conditions. These observations confirm the results from the filtration experiments explained above. The asphaltene particles and clusters were deposited at a higher rate in smaller filter paper membranes such as 50 nm due to smaller pore size structure. The results showed darker colors for smaller pore size filter paper during miscible condition of gas injection. It can be concluded that miscibility impacts the asphaltene particle in crude oil significantly compared to immiscible gas injection conditions.

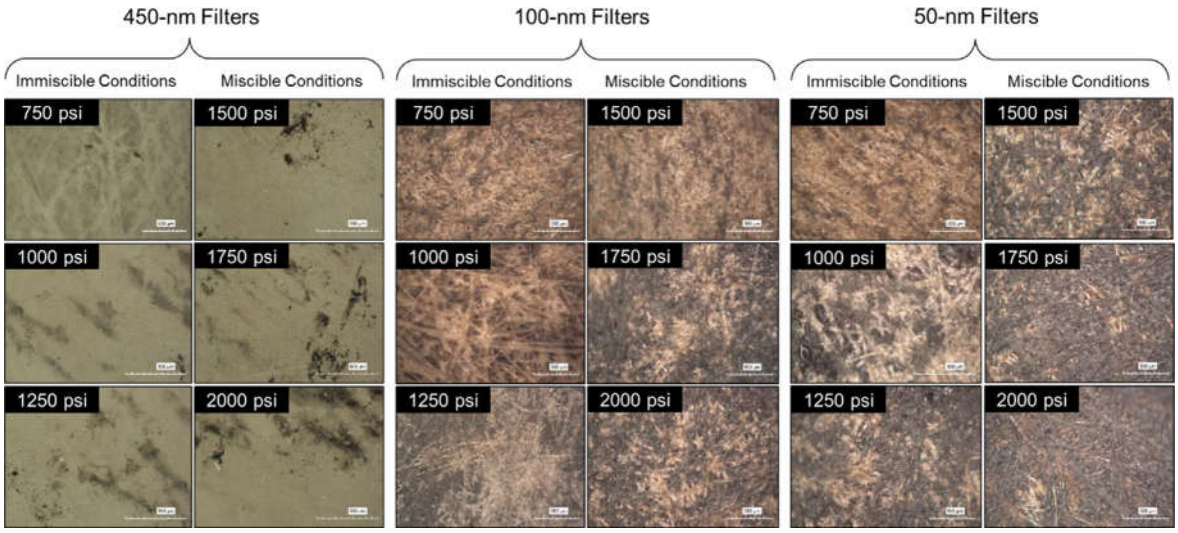

Fig. 16—Digital microscopic images (500 μm) of 450-, 100-, and 50-nm filter membranes during immiscible and miscible CO_2 injection.

SEM Analysis. To provide an advanced and clear imaging analysis of how asphaltene particles impact filter paper membranes, SEM was used to highlight the impact of pressure and asphaltene clusters on pore plugging. To illustrate this, heterogeneous filter paper membranes (i.e., 450, 100, and 50 nm) during immiscible (i.e., 1,000 psi) and miscible (i.e., 1,750 psi) CO_2 injection were selected for further imaging analysis. **Fig. 17** shows SEM images (10 μm) of the filter membrane's pore structure for 450-, 100-, and 50-nm filters using miscible injection pressures of 1,750 and 2,250 psi, respectively, at 32°C. For 450-nm filter membrane, the structure of the filter showed some asphaltene particles, which were colored black for both pressures. The structure of the 450-nm filter was slightly clearer because it has large pore size compared to 100- and 50-nm filters. As the pore size decreased, the structure of the filters was darker and fewer details could be observed due to smaller pore size, especially in 50-nm filter papers. Large area of 100-nm filter paper was impacted by asphaltene clusters, and this can be observed on the darker color, especially for miscible pressure of 1,750 psi. For the 50-nm filter

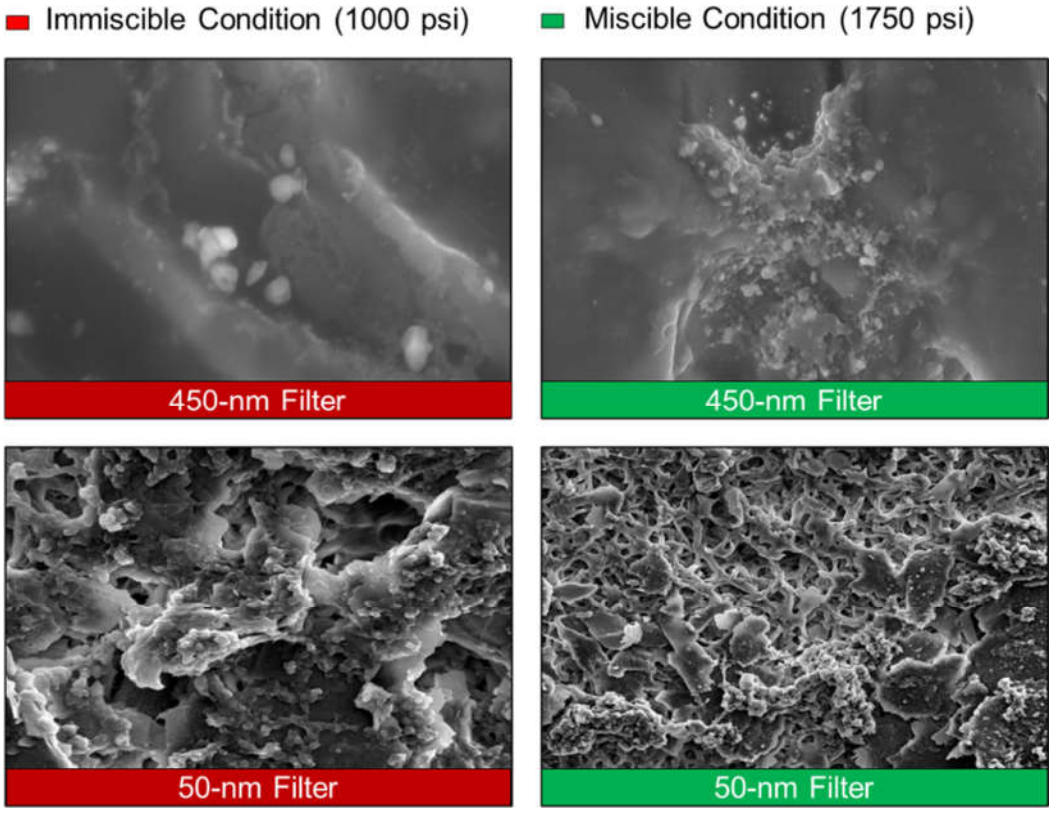

Fig. 17—SEM images (10 μm) of 450- and 50-nm filter membranes at 1,000- and 1,750-psi injection pressures.

membranes, most of the image area for both immiscible and miscible conditions was impacted by asphaltene deposition due to small pore size. These findings reveal that asphaltene particles plugged a high percentage of the filter paper's area, which was observed clearly in smaller pore size filters and high CO_2 pressure.

Pore Size Reduction Due to Asphaltene Deposition. SEM images were processed using advanced computer software to determine the pore size distribution of all filter membranes and to highlight the impact of asphaltene clusters on pore plugging. All heterogeneous filter membranes were selected for further analysis of immiscible pressure of 1,000 psi and miscible pressure of 1,750 psi experiments at 32°C. **Fig. 18a** compares the pore size distribution in the 450-nm filter membrane after CO_2 injections at 1,000 and 1,750 psi. The major distribution of the pore size of filters ranged from 40 to 300 nm at immiscible pressure of 1,000 psi but 20 to 180 nm at miscible pressure of 1,750 psi. The results showed that miscibility significantly impacted the pore size compared to immiscible conditions because higher pressure induced the asphaltene particles at higher rate and thus plugged pore membranes, which led to reduced pore sizes. When the asphaltene deposited inside the membranes, the oil was not able to pass through the filter easily due to pore plugging. These observations were found in 50-nm filter membranes. For the 50-nm filter membrane, the pore size distribution estimated to be between 1 to 7 nm for immiscible pressure (i.e., 1,000 psi) and from 0.25 to 3 nm for miscible pressure (i.e., 1,750 psi), as shown in **Fig. 18b**. Due to smaller pore size structure, a smaller pore size distribution was determined in the 50-nm filter membrane. The asphaltene clusters and particles deposited much more in 50-nm filter membranes for both immiscible and miscible pressure conditions due to smaller pore size, which led to more plugging of the pores. Su et al. (2021) developed an integrated simulation approach to predict permeability reduction under asphaltene particle aggregation and deposition. They concluded that the longer the aggregation time, the higher the flow velocity, and larger precipitation concentrations will lead to a faster reduction in permeability. These findings indicate that CO_2 injection can affect asphaltenes in crude oil during both immiscible and miscible conditions, causing significant pore blockage, especially in reservoirs with small pores, such as those found in unconventional reservoirs.

CO_2 vs. N_2 Discussion. This section is a holistic comparison discussion on how asphaltene deposition process differs under CO_2 and N_2 gas injections. The results in this research will be compared to the previous work using miscible and immiscible N_2 injection (Elturki and Imqam 2021a, 2022a). The MMP of N_2 was determined to be 1,600 psi. CO_2 and N_2 could impact the asphaltene particles in crude oil at various degrees of fluctuations. **Fig. 19** shows the asphaltene weight precent during immiscible CO_2 and N_2 injection. The results show that CO_2 impacted the asphaltene particles significantly compared to immiscible N_2 injection condition. For example, the asphaltene weight percent during 1,000 psi N_2 injection pressure on 450-nm filter was 2.52%, but for 1,000 psi CO_2 injection it was 10.90%, indicating that CO_2 had influenced the asphaltene much more than N_2. For the 50-nm filter, more asphaltene particles were trapped due to small pore size resulting in asphaltene weight percent up to 8.14 and 13.44% for N_2 and CO_2, respectively, during 1,000 -psi injection. This can be explained as the mass transfer of CO_2 is higher than N_2 due to the supercritical of CO_2 can be attained easily (Wang et al. 2018). Higher pressure led to more asphaltene precipitation and deposition in all filter membranes. To make a better comparison, **Fig. 20** shows the miscible condition results of CO_2 and N_2 on asphaltene stability. It is apparent from the figure that miscibility or near-miscible conditions of both gases led to higher asphaltene rates. For example, during miscible pressure of 1,750 psi, the asphaltene weight percent determinations were 17.33 and 26.26% on 50-nm filter for N_2 and CO_2, respectively. Higher pressure will break the bonds between the asphaltene and resins in the crude oil at higher degrees and thus will lead to more asphaltene fluctuations and deposition. Also, the

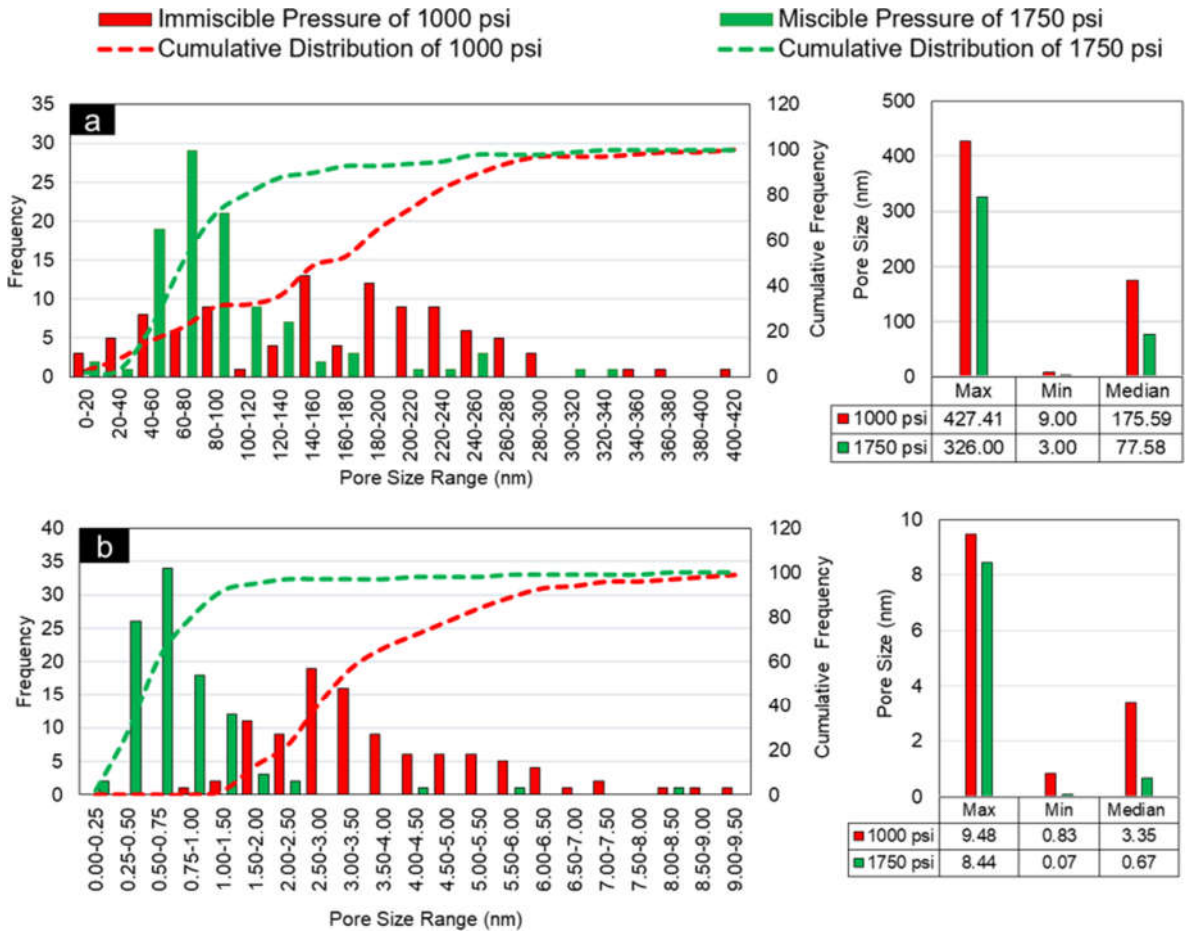

Fig. 18—Comparison of the estimated pore size distribution in (a) 450- and (b) 50-nm filter membranes after CO_2 injections of 1,000 and 1,750 psi.

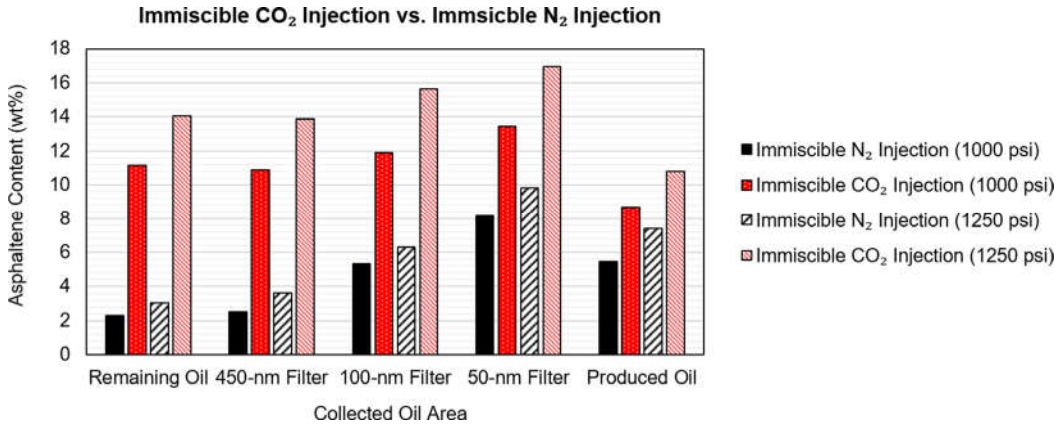

Fig. 19—Comparison of asphaltene weight percent during immiscible N_2 injection (Elturki and Imqam 2021a) and immiscible CO_2 injection pressure.

solubility of CO_2 is higher than N_2 and thus N_2 has a weak mass transfer. This could lead to poor extraction process of light hydrocarbons of crude oil and thus less asphaltene flocculation compared to CO_2. Also, CO_2 and asphaltene both have polar molecules, which lead to higher interaction rate and thus higher asphaltene deposition (Dashti et al. 2020). In terms of CO_2 and crude oil chemical interactions, the stability of asphaltenes in crude oil can be considerably impacted when they react with CO_2 and create amide functional groups. The aggregation of asphaltenes during CO_2 injection would increase during the formation of the amide functional group due to the hydrogen bonding and metal coordination reaction that may occur through this group (Afra et al. 2020). These results illustrate both effects of miscible and immiscible conditions of CO_2 and N_2, in which CO_2 is more advantageous in terms of reaching miscibility more easily. This could result in a high oil recovery but could lead to more asphaltene issues during gas injection process in real reservoirs.

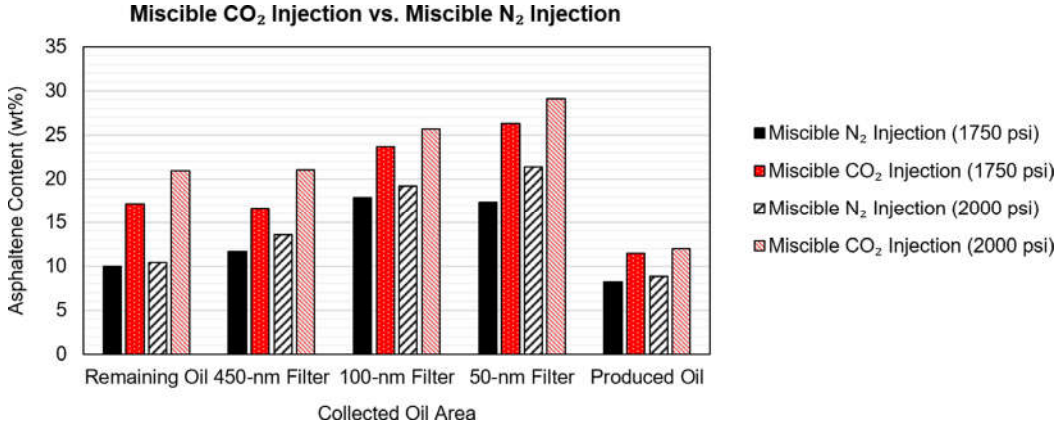

Fig. 20—Comparison of asphaltene weight percent during miscible N_2 injection (Elturki and Imqam 2022a) and miscible CO_2 injection pressure.

Conclusions

This research provided a comprehensive experimental investigation of the impact of immiscible and miscible CO_2 injection on asphaltene stability in crude oil using nanopore structure which represents unconventional reservoirs. The filtration technique was used to conduct the experiments. A slimtube was used to determine the MMP of CO_2. Various factors were studied including immiscible pressure, miscible pressure, temperature, filter membrane distribution, and pore size. The following conclusions can be drawn:

- The filtration experiments showed that the asphaltene weight percent increased as the CO_2 injection pressure increased because the greater pressure breaks the resins around the asphaltenes, resulting in asphaltene precipitation and deposition. These observations were significant during miscible injection pressures (i.e., 1,500, 1,750, and 2,000 psi) as miscible injections had higher solubility and strong extraction process of light components in the crude oil, resulting in more heavy oil components and asphaltenes. The severity of asphaltene deposition was higher in 50-nm filter paper membranes. Also, a soaking time of 120 minutes had higher impact on asphaltene instability compared to 60- and 10-minute soaking times.
- The advanced analysis of chromatography of the crude oil showed that miscible CO_2 injections (i.e., 1,750 and 2,000 psi) led to more intermediate and high components of crude oil compared to immiscible conditions (i.e., 750 psi and 1,250 psi). Also, microscopy and SEM advanced imaging revealed the impact of asphaltene accumulation on pore clogging. The results showed that when the pressure increased, pore clogging increased along with a reduction in pore size, especially in 50-nm filter paper membranes.
- The ability of CO_2 to extract light hydrocarbon components from crude oil under the same injection pressure conditions is significantly larger than in our previous work (Elturki and Imqam 2021a, 2022a), which used N_2 gas injection pressure, resulting in a significant asphaltene weight percent.

Acknowledgments

The authors would like to acknowledge the National Science Foundation, Chemical, Biological, Environmental, and Transport systems for funding the work under grant no. CBET-1932965.

References

Abutaqiya, M. I. L., Sisco, C. J., and Vargas, F. M. 2019. A Linear Extrapolation of Normalized Cohesive Energy (LENCE) for Fast and Accurate Prediction of the Asphaltene Onset Pressure. *Fluid Phase Equilib* **483**: 52–69. https://doi.org/10.1016/j.fluid.2018.10.025.

Afra, S., Samouei, H., Golshahi, N. et al. 2020. Alterations of Asphaltenes Chemical Structure Due to Carbon Dioxide Injection. *Fuel* **272**: 117708. https://doi.org/10.1016/j.fuel.2020.117708.

Ali, S. I., Lalji, S. M., Haneef, J. et al. 2021. Critical Analysis of Different Techniques Used to Screen Asphaltene Stability in Crude Oils. *Fuel* **299**: 120874. https://doi.org/10.1016/j.fuel.2021.120874.

Alimohammadi, S., Sayyad Amin, J., and Nikooee, E. 2017. Estimation of Asphaltene Precipitation in Light, Medium and Heavy Oils: Experimental Study and Neural Network Modeling. *Neural Comput & Applic* **28** (4): 679–694. https://doi.org/10.1007/s00521-015-2097-3.

Alimohammadi, S., Zendehboudi, S., and James, L. 2019. A Comprehensive Review of Asphaltene Deposition in Petroleum Reservoirs: Theory, Challenges, and Tips. *Fuel* **252**: 753–791. https://doi.org/10.1016/j.fuel.2019.03.016.

Alizadeh, A., Nakhli, H., Kharrat, R. et al. 2011. An Experimental Investigation of Asphaltene Precipitation During Natural Production of Heavy and Light Oil Reservoirs: The Role of Pressure and Temperature. *Pet Sci Technol***29** (10): 1054–1065. https://doi.org/10.1080/10916460903530531.

Altawati, F. S. 2016. An Experimental Study of the Effect of Water Saturation on Cyclic N2 and CO2 Injection in Shale Oil Reservoir. Master TThesis. Texas: Texas Tech University. http://hdl.handle.net/2346/68030.

Alves, C. A., Romero Yanes, J. F., Feitosa, F. X. et al. 2019. Effect of Temperature on Asphaltenes Precipitation: Direct and Indirect Analyses and Phase Equilibrium Study. *Energy Fuels* **33** (8): 6921–6928. https://doi.org/10.1021/acs.energyfuels.9b00408.

Amao, A. M., Siddiqui, S., Menouar, H. et al. 2012. A New Look at the Minimum Miscibility Pressure (MMP) Determination from Slimtube Measurements. Paper presented at the SPE Improved Oil Recovery Symposium, Tulsa, Oklahoma, USA, 14–18 April. SPE-153383-MS. https://doi.org/10.2118/153383-MS.

Behbahani, T. J., Ghotbi, C., Taghikhani, V. et al. 2011. Experimental Investigation and Thermodynamic Modeling of Asphaltene Precipitation. *Scientia Iranica* **18** (6): 1384–1390. https://doi.org/10.1016/j.scient.2011.11.006.

Biheri, G. and Imqam, A. 2020. Proppant Transport by High Viscosity Friction Reducer and Guar Linear Gel-Based Fracture Fluids. Paper presented at the 54th US Rock Mechanics/Geomechanics Symposium, Virtual, 28 June–1 July. ARMA-2020-1221.

Biheri, G. and Imqam, A. 2021a. Settling of Spherical Particles in High Viscosity Friction Reducer Fracture Fluids. *Energies (Basel)* **14** (9): 2462. https://doi.org/10.3390/en14092462.

Biheri, G. and Imqam, A. 2021b. Proppant Transport Using High-Viscosity Friction Reducer Fracture Fluids at High-Temperature Environment. *SPE J*. **27** (1): 60–76. SPE-206750-PA. https://doi.org/10.2118/206750-PA.

Biheri, G. and Imqam, A. 2021c. Experimental Study: High Viscosity Friction Reducer Fracture Fluid Rheological Advantages Over the Guar Linear Gel. Paper presented at the 55th US Rock Mechanics/Geomechanics Symposium, Virtual, 18–25 June. ARMA-2021-1814.

Branco, V. A. M., Mansoori, G. A., De Almeida Xavier, L. C. et al. 2001. Asphaltene Flocculation and Collapse from Petroleum Fluids. *J Pet Sci Eng* **32** (2–4): 217–230. https://doi.org/10.1016/S0920-4105(01)00163-2.

Cao, M. and Gu, Y. 2013. Oil Recovery Mechanisms and Asphaltene Precipitation Phenomenon in Immiscible and Miscible CO2 Flooding Processes. *Fuel* **109**: 157–166. https://doi.org/10.1016/j.fuel.2013.01.018.

Carvalhal, A. S., Costa, G. M. N., and Vieira de Melo, S. A. B. 2021. Full Factorial Sensitivity Analysis of Asphaltene Precipitation and Deposition in CO2 and CH4 Coreflooding. *J Pet Sci Eng* **197**: 108098. https://doi.org/10.1016/j.petrol.2020.108098.

Chandio, Z. A., Ramasamy, M., and Mukhtar, H. B. 2015. Temperature Effects on Solubility of Asphaltenes in Crude Oils. *Chem Eng Res Des* **94**: 573–583. https://doi.org/10.1016/j.cherd.2014.09.018.

Chung, T. H. 1992. Thermodynamic Modeling for Organic Solid Precipitation. Paper presented at the SPE Annual Technical Conference and Exhibition, Washington, D.C, USA, 4–7 October. SPE-24851-MS. https://doi.org/10.2118/24851-MS.

Dashti, H., Zanganeh, P., Kord, S. et al. 2020. Mechanistic Study to Investigate the Effects of Different Gas Injection Scenarios on the Rate of Asphaltene Deposition: An Experimental Approach. *Fuel* **262**: 116615. https://doi.org/10.1016/j.fuel.2019.116615.

Ekundayo, J. M. and Ghedan, S. G. 2013. Minimum Miscibility Pressure Measurement with Slim Tube Apparatus - How Unique Is the Value? Paper presented at the SPE Reservoir Characterization and Simulation Conference and Exhibition, Abu Dhabi, UAE, 16–18 September. SPE-165966-MS. https://doi.org/10.2118/165966-MS.

Elturki, M. and Imqam, A. 2020a. High Pressure-High Temperature Nitrogen Interaction with Crude Oil and Its Impact on Asphaltene Deposition in Nano Shale Pore Structure: An Experimental Study. Paper presented at the SPE/AAPG/SEG Unconventional Resources Technology Conference, Virtual, 20–22 July. URTEC-2020-3241-MS. https://doi.org/10.15530/urtec-2020-3241.

Elturki, M. and Imqam, A. 2020b. Application of Enhanced Oil Recovery Methods in Unconventional Reservoirs: A Review and Data Analysis. Paper presented at the 54th US Rock Mechanics/Geomechanics Symposium, Virtual, 28 June–1 July. ARMA-2020-1081.

Elturki, M. and Imqam, A. 2021a. Asphaltene Thermodynamic Flocculation during Immiscible Nitrogen Gas Injection. *SPE J*. **26** (5): 3188–3204. SPE-206709-PA. https://doi.org/10.2118/206709-PA.

Elturki, M. and Imqam, A. 2021b. An Experimental Study Investigating the Impact of Miscible and Immiscible Nitrogen Injection on Asphaltene Instability in Nano Shale Pore Structure. Paper presented at the SPE International Conference on Oilfield Chemistry, The Woodlands, Texas, USA, 6–7 December. SPE-204294-MS. https://doi.org/10.2118/204294-MS.

Elturki, M. and Imqam, A. 2021c. Analysis of Nitrogen Minimum Miscibility Pressure MMP and Its Impact on Instability of Asphaltene Aggregates - An Experimental Study. Paper presented at the SPE Trinidad and Tobago Section Energy Resources Conference, Virtual, 28–30 June. SPE-200900-MS. https://doi.org/10.2118/200900-MS.

Elturki, M. and Imqam, A. 2022a. Asphaltene Thermodynamic Precipitation during Miscible Nitrogen Gas Injection. *SPE J*. **27** (1): 877–894. SPE-208588-PA. https://doi.org/10.2118/208588-PA.

Elturki, M. and Imqam, A. 2022b. An Experimental Investigation of Asphaltene Aggregation Under Carbon Dioxide Injection Flow in Ultra-Low-Permeability Pore Structure. Paper presented at the SPE Canadian Energy Technology Conference, Calgary, Alberta, Canada, 16–17 March. SPE-208950-MS. https://doi.org/10.2118/208950-MS.

Elturki, M., McElroy, P. D., Li, D. et al. 2021. Simulation Study Investigating the Impact of Carbon Dioxide Foam Fracturing Fluids on Proppant Transport. Paper presented at the SPE Trinidad and Tobago Section Energy Resources Conference, Virtual, 28–30 June. SPE-200950-MS. https://doi.org/10.2118/200950-MS.

Elwegaa, K. and Emadi, H. 2019. Improving Oil Recovery from Shale Oil Reservoirs Using Cyclic Cold Nitrogen Injection – An Experimental Study. *Fuel* **254**: 115716. https://doi.org/10.1016/j.fuel.2019.115716.

Espinoza Mejia, J. E., Li, X., and Zheng, R. 2022. Experimental Study of Asphaltene Precipitation and Deposition During Immiscible CO2 - EOR Process. Paper presented at the SPE International Conference and Exhibition on Formation Damage Control, Lafayette, Louisiana, USA, 23–24 February. SPE-208802-MS. https://doi.org/10.2118/208802-MS.

Fakher, S. and Imqam, A. 2018. Investigating and Mitigating Asphaltene Precipitation and Deposition in Low Permeability Oil Reservoirs During Carbon Dioxide Flooding to Increase Oil Recovery. Paper presented at the SPE Annual Caspian Technical Conference and Exhibition, Astana, Kazakhstan, 31 October–2 November. SPE-192558-MS. https://doi.org/10.2118/192558-MS.

Fakher, S. and Imqam, A. 2019. Asphaltene Precipitation and Deposition during CO2 Injection in Nano Shale Pore Structure and Its Impact on Oil Recovery. *Fuel* **237**: 1029–1039. https://doi.org/10.1016/j.fuel.2018.10.039.

Fakher, S. and Imqam, A. 2020. Flow of Carbon Dioxide in Micro and Nano Pores and Its Interaction with Crude Oil to Induce Asphaltene Instability. *SN Appl Sci* **2** (6): 1–13. https://doi.org/10.1007/s42452-020-2850-9.

Goual, L. 2012. *Petroleum Asphaltenes, Crude Oil Emulsions Composition Stability and Characterization*, 978–953. London: Intechopen. https://doi.org/10.5772/2677.

Guzmán, R., Rodríguez, S., Torres-Mancera, P. et al. 2020. Evaluation of Asphaltene Stability of a Wide Range of Mexican Crude Oils. *Energy Fuels* **35** (1): 408–418. https://doi.org/10.1021/acs.energyfuels.0c03301.

Hajizadeh, N., Moradi, G., and Ashoori, S. 2020. Experimental Investigation and Modelling of Asphaltene Precipitation during Gas Injection. *JChPE* **54** (2): 223–234. https://doi.org/10.22059/JCHPE.2020.291688.1299.

Hashmi, S. M. and Firoozabadi, A. 2010. Effect of Dispersant on Asphaltene Suspension Dynamics: Aggregation and Sedimentation. Paper presented at the SPE Annual Technical Conference and Exhibition, Florence, Italy, 19–22 September. SPE-135599-MS. https://doi.org/10.2118/135599-MS.

Hassanpouryouzband, A., Joonaki, E., Taghikhani, V. et al. 2017. New Two-Dimensional Particle-Scale Model To Simulate Asphaltene Deposition in Wellbores and Pipelines. *Energy Fuels* **32** (3): 2661–2672. https://doi.org/10.1021/acs.energyfuels.7b02714.

Hassanpouryouzband, A., Joonaki, E., Vasheghani Farahani, M. et al. 2020. Gas Hydrates in Sustainable Chemistry. *Chem Soc Rev* **49** (15): 5225–5309. https://doi.org/10.1039/c8cs00989a.

Hoepfner, M. P., Limsakoune, V., Chuenmeechao, V. et al. 2013. A Fundamental Study of Asphaltene Deposition. *Energy Fuels* **27** (2): 725–735. https://doi.org/10.1021/ef3017392.

Jafari Behbahani, T., Ghotbi, C., Taghikhani, V. et al. 2012. Investigation on Asphaltene Deposition Mechanisms during CO_2 Flooding Processes in Porous Media: A Novel Experimental Study and A Modified Model Based on Multilayer Theory for Asphaltene Adsorption. *Energy Fuels* **26** (8): 5080–5091. https://doi.org/10.1021/ef300647f.

Jamaluddin, A. K. M., Joshi, N., Iwere, F. et al. 2002. An Investigation of Asphaltene Instability Under Nitrogen Injection. Paper presented at the SPE International Petroleum Conference and Exhibition in Mexico, Villahermosa, Mexico, 10–12 February. SPE-74393-MS. https://doi.org/10.2118/74393-MS.

Kar, T., Naderi, K., and Firoozabadi, A. 2020. Asphaltene Deposition and Removal in Flowlines and Mitigation by Effective Functional Molecules. *SPE J.* **25** (2): 771–787. SPE-199878-PA. https://doi.org/10.2118/199878-PA.

Khalaf, M. H. and Mansoori, G. A. 2019. Asphaltenes Aggregation during Petroleum Reservoir Air and Nitrogen Flooding. *J Pet Sci Eng* **173**: 1121–1129. https://doi.org/10.1016/j.petrol.2018.10.037.

Li, Z. and Firoozabadi, A. 2010. Cubic-Plus-Association Equation of State for Asphaltene Precipitation in Live Oils. *Energy Fuels* **24** (5): 2956–2963. https://doi.org/10.1021/ef9014263.

Liu, J., Sheng, J. J., Emadibaladehi, H. et al. 2021. Experimental Study of the Stimulating Mechanism of Shut-in after Hydraulic Fracturing in Unconventional Oil Reservoirs. *Fuel* **300**: 120982. https://doi.org/10.1016/j.fuel.2021.120982.

Luo, P., Luo, W., and Li, S. 2017. Effectiveness of Miscible and Immiscible Gas Flooding in Recovering Tight Oil from Bakken Reservoirs in Saskatchewan, Canada. *Fuel* **208**: 626–636. https://doi.org/10.1016/j.fuel.2017.07.044.

Madhi, M., Kharrat, R., and Hamoule, T. 2018. Screening of Inhibitors for Remediation of Asphaltene Deposits: Experimental and Modeling Study. *Petroleum* **4** (2): 168–177. https://doi.org/10.1016/j.petlm.2017.08.001.

Melendez-Alvarez, A. A., Garcia-Bermudes, M., Tavakkoli, M. et al. 2016. On the Evaluation of the Performance of Asphaltene Dispersants. *Fuel* **179**: 210–220. https://doi.org/10.1016/j.fuel.2016.03.056.

Milad, M., Junin, R., Sidek, A. et al. 2021. Huff-n-Puff Technology for Enhanced Oil Recovery in Shale/Tight Oil Reservoirs: Progress, Gaps, and Perspectives. *Energy Fuels* **35** (21): 17279–17333. https://doi.org/10.1021/acs.energyfuels.1c02561.

Mohammadi, S., Rashidi, F., Mousavi-Dehghani, S. A. et al. 2016. On the Effect of Temperature on Precipitation and Aggregation of Asphaltenes in Light Live Oils. *Can J Chem Eng* **94** (9): 1820–1829. https://doi.org/10.1002/cjce.22555.

Mohammed, I., Mahmoud, M., Al Shehri, D. et al. 2021. Asphaltene Precipitation and Deposition: A Critical Review. *J Pet Sci Eng* **197**: 107956. https://doi.org/10.1016/j.petrol.2020.107956.

Moradi, S., Dabir, B., Rashtchian, D. et al. 2012. Effect of Miscible Nitrogen Injection on Instability, Particle Size Distribution, and Fractal Structure of Asphaltene Aggregates. *J Dispers Sci Technol* **33** (5): 763–770. https://doi.org/10.1080/01932691.2011.567878.

Nascimento, F. P., Pereira, V. J., Souza, R. P. et al. 2021. An Experimental and Theoretical Investigation of Asphaltene Precipitation in a Crude Oil from the Brazilian Pre-Salt Layer under CO2 Injection. *Fuel* **284**: 118968. https://doi.org/10.1016/j.fuel.2020.118968.

Negahban, S., Bahamaish, J. N. M., Joshi, N. et al. 2005. An Experimental Study at an Abu Dhabi Reservoir of Asphaltene Precipitation Caused By Gas Injection. *SPE Prod & Fac* **20** (2): 115–125. SPE-80261-PA. https://doi.org/10.2118/80261-PA.

Pereira, J. C., López, I., Salas, R. et al. 2007. Resins: The Molecules Responsible for the Stability/Instability Phenomena of Asphaltenes. *Energy Fuels* **21** (3): 1317–1321. https://doi.org/10.1021/ef0603333.

Punase, A., Prakoso, A., and Hascakir, B. 2016. The Polarity of Crude Oil Fractions Affects the Asphaltenes Stability. Paper presented at the SPE Western Regional Meeting, Anchorage, Alaska, USA, 23–26 May. SPE-180423-MS. https://doi.org/10.2118/180423-MS.

Shahriar, M. 2014. The Aggregation of Asphaltene Molecules as a Function of Carbon Dioxide Concentration. PhD dissertation. Texas: Texas Tech University. https://hdl.handle.net/2346/87013.

Sheng, J. J. 2015. Enhanced Oil Recovery in Shale Reservoirs by Gas Injection. *J Nat Gas Sci Eng* **22**: 252–259. https://doi.org/10.1016/j.jngse.2014.12.002.

Shen, Z. and Sheng, J. J. 2017. Experimental Study of Permeability Reduction and Pore Size Distribution Change Due to Asphaltene Deposition during CO_2 Huff and Puff Injection in Eagle Ford Shale. *Asia-Pac J Chem Eng* **12** (3): 381–390. https://doi.org/10.1002/apj.2080.

Shen, Z. and Sheng, J. J. 2018. Experimental and Numerical Study of Permeability Reduction Caused by Asphaltene Precipitation and Deposition during CO2 Huff and Puff Injection in Eagle Ford Shale. *Fuel* **211**: 432–445. https://doi.org/10.1016/j.fuel.2017.09.047.

Shi, B., Song, S., Chen, Y. et al. 2021. Status of Natural Gas Hydrate Flow Assurance Research in China: A Review. *Energy Fuels* **35** (5): 3611–3658. https://doi.org/10.1021/acs.energyfuels.0c04209.

Soroush, S., Pourafshary, P., and Vafaie-Sefti, M. 2014. A Comparison of Asphaltene Deposition in Miscible and Immiscible Carbon Dioxide Flooding in Porous Media. Paper presented at the SPE EOR Conference at Oil and Gas West Asia, Muscat, Oman, 31 March–2 April. SPE-169657-MS. https://doi.org/10.2118/169657-MS.

Su, X., Moghanloo, R. G., Qi, M. et al. 2021. An Integrated Simulation Approach To Predict Permeability Impairment under Simultaneous Aggregation and Deposition of Asphaltene Particles. *SPE J.* **26** (2): 959–972. SPE-205028-PA. https://doi.org/10.2118/205028-PA.

Syed, F. I., Neghabhan, S., Zolfaghari, A. et al. 2020. Numerical Validation of Asphaltene Precipitation and Deposition during CO2 Miscible Flooding. *Petroleum Research* **5** (3): 235–243. https://doi.org/10.1016/j.ptlrs.2020.04.002.

Tavakkoli, M., Panuganti, S. R., Taghikhani, V. et al. 2014. Precipitated Asphaltene Amount at High-Pressure and High-Temperature Conditions. *Energy Fuels* **28** (3): 1596–1610. https://doi.org/10.1021/ef401074e.

Wang, P., Zhao, F., Hou, J. et al. 2018. Comparative Analysis of CO2, N2, and Gas Mixture Injection on Asphaltene Deposition Pressure in Reservoir Conditions. *Energies (Basel)* **11** (9): 2483. https://doi.org/10.3390/en11092483.

Zanganeh, P., Ayatollahi, S., Alamdari, A. et al. 2012. Asphaltene Deposition during CO_2 Injection and Pressure Depletion: A Visual Study. *Energy Fuels* **26** (2): 1412–1419. https://doi.org/10.1021/ef2012744.

Zanganeh, P., Dashti, H., and Ayatollahi, S. 2018. Comparing the Effects of CH4, CO2, and N2 Injection on Asphaltene Precipitation and Deposition at Reservoir Condition: A Visual and Modeling Study. *Fuel* **217**: 633–641. https://doi.org/10.1016/j.fuel.2018.01.005.

Zheng, T., Yang, Z., Liu, X. et al. 2021. Understanding Immiscible Natural Gas Huff-N-Puff Seepage Mechanism in Porous Media: A Case Study of CH4 Huff-N-Puff by Laboratory Numerical Simulations in Chang-7 Tight Core. *Nat Resour Res* **30** (3): 2397–2411. https://doi.org/10.1007/s11053-021-09836-2.

Zoback, M. D. and Kohli, A. H. 2019. *Unconventional Reservoir Geomechanics*. Cambridge: Cambridge University Press. https://doi.org/10.1017/9781316091869.

Zolghadr, A., Escrochi, M., and Ayatollahi, S. 2013. Temperature and Composition Effect on CO_2 Miscibility by Interfacial Tension Measurement. *J Chem Eng Data* **58** (5): 1168–1175. https://doi.org/10.1021/je301283e.